



## Structural Characterization and Ordering Transformation of Mechanically Alloyed Nanocrystalline Fe-28Al Powder

Lima Amiri Talischi<sup>1</sup>, Ahad Samadi<sup>2</sup>

<sup>1</sup>Department of Materials Engineering, Sahand University of Technology, P.O.Box 51335-1996, Tabriz, Iran.

Received: 11 May 2016; Accepted: 19 September 2016

Corresponding author email: [samadi@sut.ac.ir](mailto:samadi@sut.ac.ir)

### ABSTRACT

The synthesis of nanocrystalline Fe<sub>3</sub>Al powder by mechanical alloying as well as the structural ordering of the synthesized Fe<sub>3</sub>Al particles during the subsequent thermal analysis were investigated. Mechanical alloying was performed up to 100 hours using a planetary ball mill apparatus with rotational speed of 300 rpm under argon atmosphere at ambient temperature. The synthesized powders were characterized using X-ray diffraction, SEM observations and differential scanning calorimetry (DSC). The results show that the A2-type Fe<sub>3</sub>Al with disordered bcc structure is only formed after 70 hours milling. The corresponding lattice strain, mean crystallite and particle sizes for the 70 hours milled Fe<sub>3</sub>Al powder were determined as 2.5%, 10 and 500 nm, respectively. The subsequent heating during DSC causes a DO<sub>3</sub>-type Fe<sub>3</sub>Al ordering in 70 and 100 hours milled powders, however in 40 hours milled powder it only assists for the formation of disordered solid solution. Longer milling time induces a large amount of lattice strain in Fe<sub>3</sub>Al powder particles and consequently facilitates the atomic diffusion thus decreases the activation energy of ordering. The activation energy for ordering transformation of 100 hours Fe<sub>3</sub>Al milled powder was calculated as 152.1 kJ/mole which is about 4 kJ/mole lower than that for 70 hours milled powder.

**Keywords:** Fe<sub>3</sub>Al intermetallic compound; Mechanical alloying; Nanocrystalline powder; X-ray diffraction, Ordering.

How to cite this article:

Amiri Talischi L, Samadi A, Structural Characterization and Ordering Transformation of Mechanically Alloyed Nanocrystalline Fe-28Al Powder. *J Ultrafine Grained Nanostruct Mater*, 2016; 49(2):112-119.

DOI: [10.7508/jufgnsnm.2016.02.09](https://doi.org/10.7508/jufgnsnm.2016.02.09)

### 1. Introduction

Fe<sub>3</sub>Al (Fe-28 at.% Al) is one of the intermetallic compounds which due to its interesting properties has been widely studied by the materials researchers. In addition to disordered bcc structure at temperatures higher than 800°C, it has two ordered structures including B2 (between 550-800°C) and DO<sub>3</sub> (below 550°C) [1].

Fe<sub>3</sub>Al owing to its excellent corrosion resistance in oxidizing and sulfidizing environments, low

density, high elastic modulus and lower cost has shown adequate potentials for many structural applications such as gas metal filters and heating elements [2-5]. However, the brittleness at ambient temperature has limited its applications [1, 5, 6]. So many attempts have been employed to improve the ductility of Fe<sub>3</sub>Al intermetallic via controlling the chemical composition, microstructural modifications and improvement of fabrication methods [7-12]. Grain refining is one

of these attempts which through dissemination of microstructural grain boundaries can suspend the propagation of micro cracks. Also it decreases the anti-phase boundaries (APBs) energy thus facilitates the slip of super-dislocations [12, 13]. Since the mechanical alloying is a capable technique in synthesis of nanocrystalline materials, a wide attention has been paid to the use of this technique in synthesis of fine structured intermetallics [9-12, 14-16]. Apart from all capabilities of mechanical alloying in disordering the lattice structure and grain refining of the brittle intermetallics like Fe<sub>3</sub>Al, it is also flexibly controlled and reasonably low-cost [16]. So in this article, in addition to synthesize the nanocrystalline Fe<sub>3</sub>Al by mechanical alloying and its characterization, DO<sub>3</sub>-type ordering of the synthesized Fe<sub>3</sub>Al powder is studied during the subsequent heating.

## 2. Materials and Methods

The elemental pure powders of iron (99.5% purity) and aluminum (99% purity) were used as raw materials for mechanical alloying of Fe-28 at.% Al, i.e. Fe<sub>3</sub>Al, intermetallic. The mechanical alloying was carried out using a planetary ball mill laboratory apparatus, manufactured by an Iranian company named as Asia Sanat Rakhsh, under argon atmosphere at ambient temperature. The rotational speed of the ball mill and the ball to powder weight ratio was considered as 300 rpm and 10:1, respectively. The balls diameter was 10 and 15 mm. In order to reduce the effect of cold welding 0.5 wt.% stearic acid was added to the powder mixture. The powders were milled up to 100 hours then the synthesized powders were withdrawn from the cups after a few time intervals. Phase analysis and structural investigations for determination of lattice parameter, crystallite size and internal strain of the powders were carried out by X-ray diffraction (XRD) technique using Cu-k<sub>α</sub> radiation in a Bruker-Axe diffractometer model advanced D8. The lattice parameter of Fe-28 at.% Al powder at different milling times was calculated by equation (1) called as Nelson-Riley [17] equation, where  $a$  is the lattice parameter which is calculated for each of the appeared peaks in the XRD pattern of the sample,  $a_0$  is the true value of lattice parameter,  $\theta$  is the diffraction angle and  $k$  is a constant. The term  $(\cos\theta^2/\sin\theta + \cos\theta^2/\theta)$  is called as the Nelson-Riley function. If the value of  $a$  is plotted against the Nelson-Riley (N-R) function, a straight line will be resulted which by extrapolating

it to  $\cos\theta^2=0$  the value of  $a_0$  is obtained.

$$a = a_0 + a_0 k \left( \frac{\cos\theta^2}{\sin\theta} + \frac{\cos\theta^2}{\theta} \right) \quad (\text{eq. 1})$$

In order to separate the contribution of the crystallite size and internal strain of the powders on the broadening of XRD peaks, the Williamson-Hall [18] method was used as equation (2).

$$\beta \cos\theta = \frac{\lambda}{D} + 4 \epsilon \sin\theta \quad (\text{eq. 2})$$

In this equation,  $\beta$  is integral breadth,  $\lambda$  is the radiation wavelength of the used X-ray,  $\theta$  is diffraction angle,  $D$  is the average crystallite size and  $\epsilon$  is the internal strain of the powders. By plotting  $\beta \cos\theta$  versus  $\sin\theta$ , the average values of crystallite sizes and internal strains can be estimated from extrapolating of the obtained line to  $\sin\theta=0$  and slope of the resultant line, respectively. Furthermore, the morphology and size of the powders were observed using scanning electron microscopy (SEM) model Cam Scan MV2300.

To track any structural changes which may be occurred during the heating of the milled powders, differential scanning calorimetry (DSC) was carried out using an apparatus model NETZSCH DSC 404 C in a temperature range of 200-600°C under a high purity argon atmosphere and heating rate of 10 K/min. In addition to determine the activation energy needed for ordering of Fe<sub>3</sub>Al, the 70 and 100 hours milled powders were DSC analyzed at different heating rates of 5, 10, 20 and 30 K/min. Then the activation energy was determined by Kissinger method [19] using equation (3):

$$\frac{d \left( \ln \frac{\alpha}{T_m^2} \right)}{d \left( \frac{1}{T_m} \right)} = - \frac{E}{R} \quad (\text{eq. 3})$$

where  $\alpha$  is heating rate of DSC,  $R$  is gas constant,  $T_m$  is peak temperature observed for corresponding ordering in DSC curves and  $E$  is the activation energy of ordering. Plotting  $\left( \ln \frac{\alpha}{T_m^2} \right)$  versus  $\left( \frac{1}{T_m} \right)$  yields a straight line which its slope, according to equation (3), give us the activation energy of the ordering.

## 3. Results and discussion

SEM images of pure Fe and Al powders have been shown in Fig. 1. As it can be seen in this figure the Al particles have irregular shape with size of 5-30  $\mu\text{m}$  and Fe particles show nearly spherical shape with less than 5  $\mu\text{m}$  sizes.

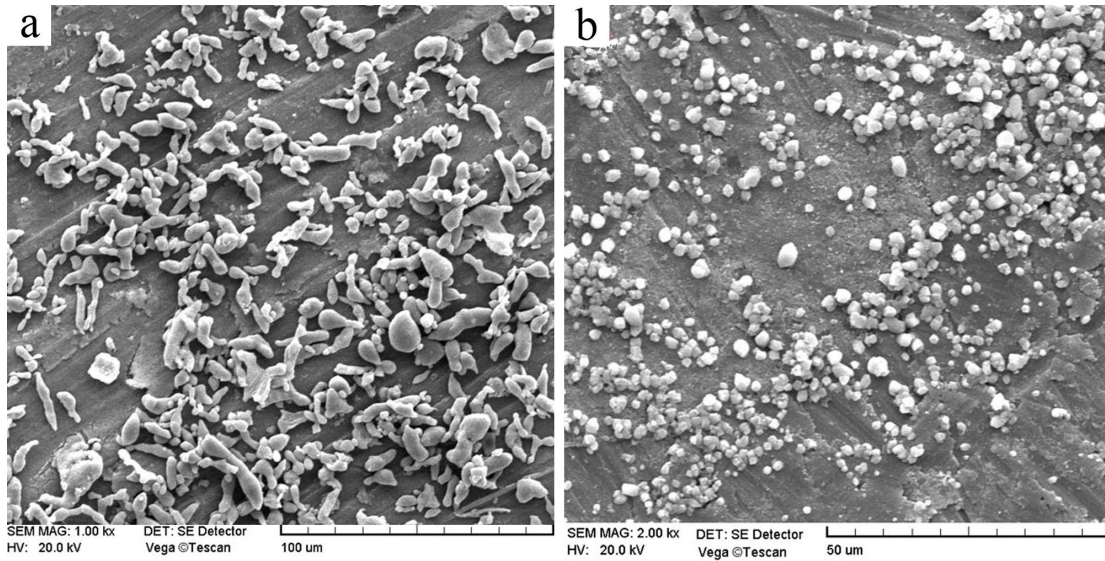


Fig. 1- SEM micrographs of pure powder of Al (a) and Fe (b).

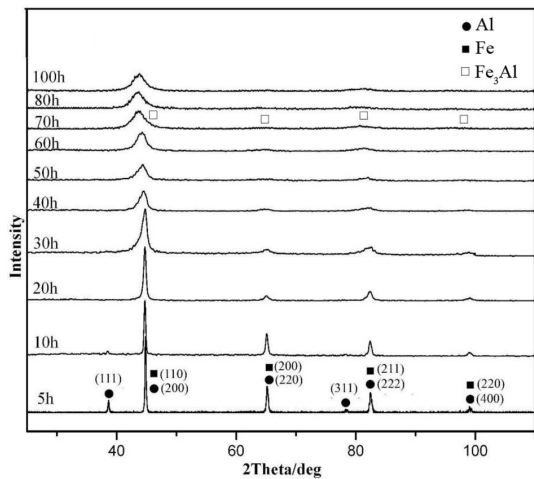


Fig. 2- XRD spectra of Fe-28 at.% Al powder after milling for different times.

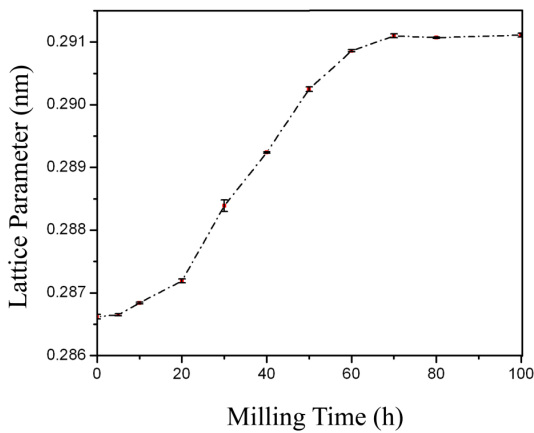


Fig. 3- The variation of lattice parameter of Fe-28 at.% Al powder as a function of milling time.

Fig. 2 illustrates the XRD spectra of milled powders after different milling times. As it can be observed the reflections of (200), (220), (222) and (400) in fcc Al have been superimposed, with the reflections of (110), (200), (211) and (220) in bcc Fe, respectively. Despite that the (111) and (311) reflections of aluminum are not superimposed with the iron peaks which clearly indicates the presence of pure aluminum in powder mixture until 20 hours milling. However by increasing the milling time to 20 hours both of (111) and (311) reflections of aluminum have been disappeared. By increasing the milling time to 70 hours, iron peaks have shifted a little to the lower angles then their positions have been fixed after 70 hours milling. Since Al atoms with atomic radius of 0.143 nm are bigger than Fe atoms with atomic radius of 0.124 nm, so dissolving of Al in Fe lattice leads to increase in the distance of the atomic planes of iron hence shifts its peaks to lower angles and increases the lattice parameter. So it seems that through milling up to 70 hours, bcc iron dissolves the aluminum atoms to form a disordered Fe(Al) solid solution, however after that the formed solid solution is saturated hence further milling up to 100 hours has no effect on the position of the reflection peaks of Fe(Al) solid solution.

The variation of the lattice parameter of bcc phase as a function of milling time has been illustrated in Fig 3. As it can be seen in this figure, while the lattice parameter of the bcc phase indicates no considerable changes in the preliminary times of milling, however its obvious changes begin after 30 hours and continue up to 70 hours milling.

The lattice parameter after 70 hours ball milling is 0.2911 nm which is nearly the same value reported by Cahn [20] for A2-type  $\text{Fe}_3\text{Al}$  compound. So it seems that after 70 hours ball milling the A2-type  $\text{Fe}_3\text{Al}$  intermetallic is formed. A2-type  $\text{Fe}_3\text{Al}$  is one of the allotropies of the  $\text{Fe}_3\text{Al}$  compound which has a disordered bcc structure. After 70 hours milling no noticeable change has occurred in lattice parameter of the formed  $\text{Fe}_3\text{Al}$ .

In Fig. 2 via increasing the milling time a progressive broadening in diffraction peaks of the synthesized powders is observed which is attributed to either the reduction of grain size or increasing the internal strain of the powders [16]. The Williamson-Hall method [18] is a technique which can separate the contribution of strain level and crystallite size refinement on the peak broadening. The lattice strain and average crystallite size of the synthesized Fe-28 at.% Al powders as a function of milling time have been separately illustrated in Fig. 4. According to this figure, by increasing the milling time the lattice strain of the powder particles has constantly increased while the average crystallite size has decreased. As it can be seen the crystallite size in the preliminary times of milling has abruptly decreased then after 40 hours milling it has followed a rather steady state behavior. The abrupt reduction in crystallite size during the preliminary times of milling, as previously reported by Karimbeigi et al. [21], is caused from severe plastic deformation of the powder particles. The longer milling times, due to inducing the higher concentration of vacancies and dislocations in powder particles, increase their lattice strains. According to Fig. 4, the lattice strain and average crystallite size of the synthesized A2-type  $\text{Fe}_3\text{Al}$  powder after 70 hours milling was calculated as 2.5% and 10 nm, respectively. So a nanocrystalline disordered  $\text{Fe}_3\text{Al}$  powder was

synthesized by mechanical alloying after 70 hours milling.

Fig. 5 shows SEM micrographs of the synthesized Fe-28 at.% Al powder particles after different milling times. In 10 hours milled powder (Fig. 5 (a)) which illustrates the metallic particles of iron and aluminum, owing to their ductility and low lattice strains, the agglomerations of flake shape particles have formed. In micrograph of this sample, the variation of particle sizes from about 15 to 5  $\mu\text{m}$  or less is observed. After 20 hours milling the particles have found a semi spherical shape. By continuing the ball milling for longer times, owing to increasing the lattice strain of the particles hence their strain hardening and brittleness, the particles have been fractured and their size has been further decreased (Fig. 5 (c-e)). The mean size of the particles in 70 hours ball milled sample, according to Fig. 5 (e), is estimated to be about 500 nm.

The synthesized powders were subjected to DSC analysis to follow their phase transformations as well as structural changes during heating. Fig. 6 illustrates the DSC curves of the 40, 70 and 100 hours milled powders. As it can be seen in this figure, all of the samples exhibit an exothermic peak at a temperature range between 330-450°C. However it should be noted that by increasing the milling time not only the released heat has noticeably decreased but also the peaks have shifted to lower temperatures. For 100 hours milled powder only a too weak exothermic peak is observed at about 360°C. To characterize the corresponding phase transformation of these exothermic peaks, the DSC analyzed powders were studied by XRD which their related spectrums have been illustrated in Fig. 7. Comparing the XRD peaks of the milled powders before DSC and after that (Fig. 2 and Fig. 7) shows clearly that the XRD

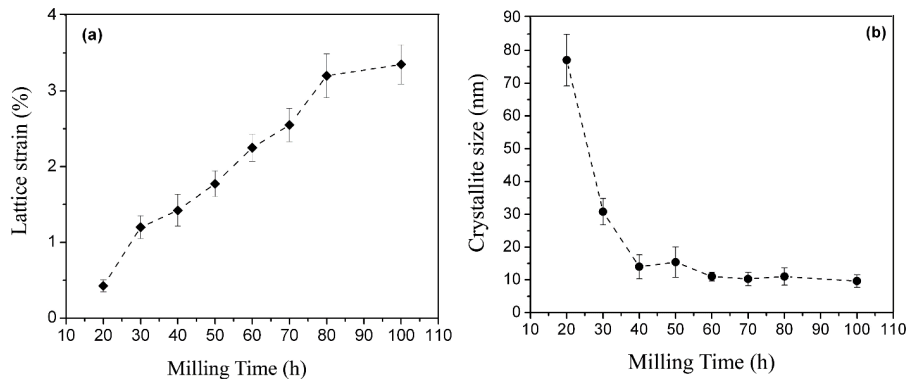


Fig. 4- Lattice strain (a) and average crystallite size (b) of the synthesized Fe-28 at.% Al powder as a function of milling time.

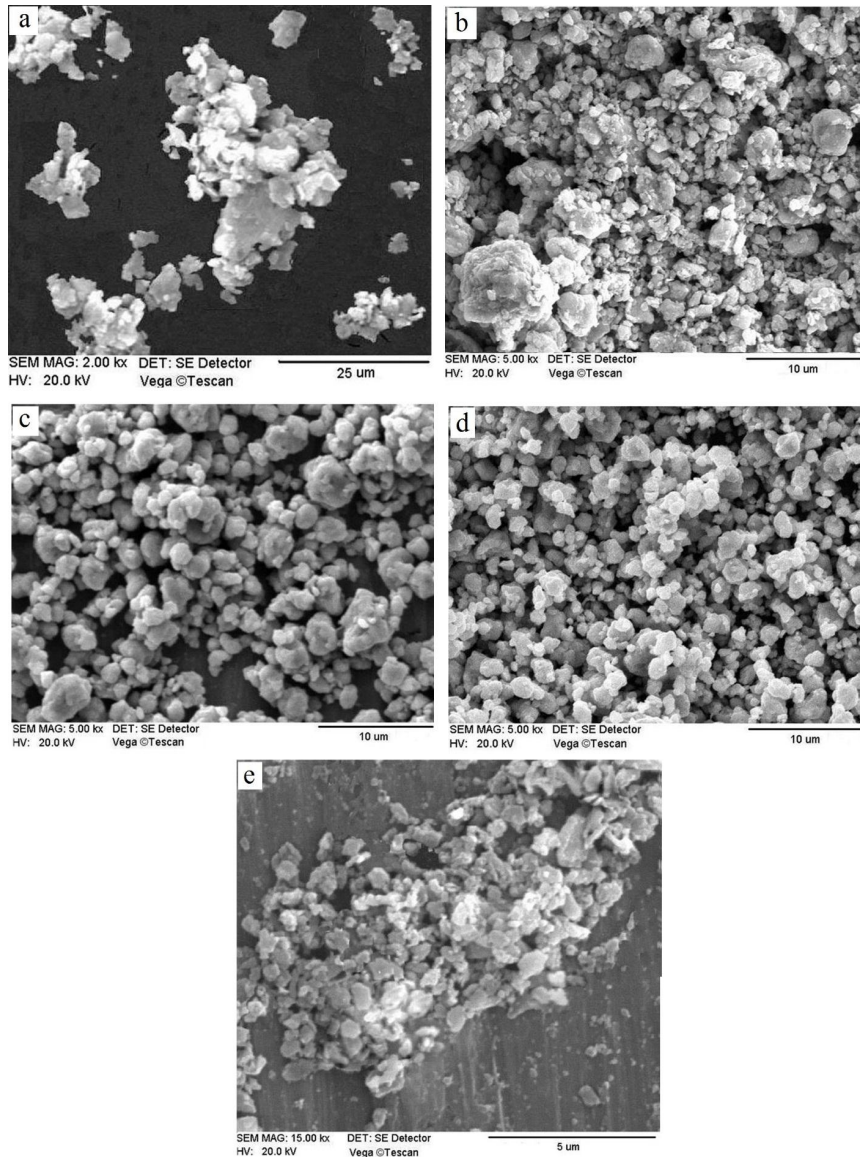


Fig. 5- SEM micrographs of Fe-28 at.% Al powder after 10 (a), 20 (b), 30 (c), 50 (d) and 70 (e) hours milling.

peaks have been sharpened in Fig. 7. This can be attributed to either grow of the grains or stress relieve of the powders during DSC heating. The mean crystallite size and lattice strain of the powders before DSC and after that have been presented in Table 1. According to this table, the influence of heating on reducing the lattice strain is more perceptible than that on the increasing of crystallite size. Such a behavior has been previously reported by Rafiei et al. [22]. As previously mentioned mechanical alloying imposes a high concentration of lattice defects such as vacancies and dislocations. During the subsequent heating through absorbing the vacancies in grain boundaries or dislocations the lattice is re-ordered hence the lattice strain as well as lattice

parameter are decreased [23]. As can be seen in Fig. 7 the  $DO_3$  super lattice reflections have been appeared for 70 and 100 hours milled powders after DSC. This indicates that during the heating of the  $Fe_3Al$  powder the bcc disordered structure has been transformed to ordered  $DO_3$  structure. The lattice parameter of 70 hours milled powder after DSC was calculated as 0.5793 nm which is in good agreement with the  $DO_3$ -type  $Fe_3Al$  lattice parameter reported by Cahn [20].

The lack of  $DO_3$  super lattice reflections for 40 hours milled powder in Fig. 7 denotes no ordering in this sample. The observed exothermic peak for 40 hours milled powder in DSC curve in Fig. 6 can be related to the thermally assisted formation of  $Fe(Al)$  solid solution

from elemental Fe and Al powders. In longer time milled powders this exothermic peak can be associated with the ordering of Fe<sub>3</sub>Al to DO<sub>3</sub>-type super lattice structure. These results are also in good agreement with Zhu and Iwasaki [24] results. Thermally activated formation of Fe(Al) solid solution as well as ordering of Fe<sub>3</sub>Al can be described via a vacancy migration mechanism based on local state strain. Internal strain enhances the vacancy migration hence improves the formation of solid

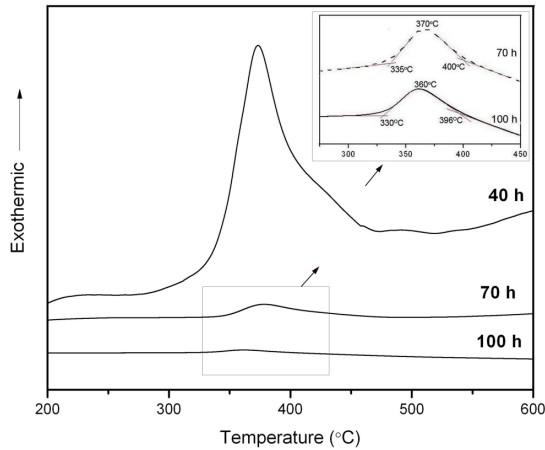


Fig. 6- DSC curves of the synthesized Fe-28 at.% Al powder in different milling times (heating rate: 10 K/min).

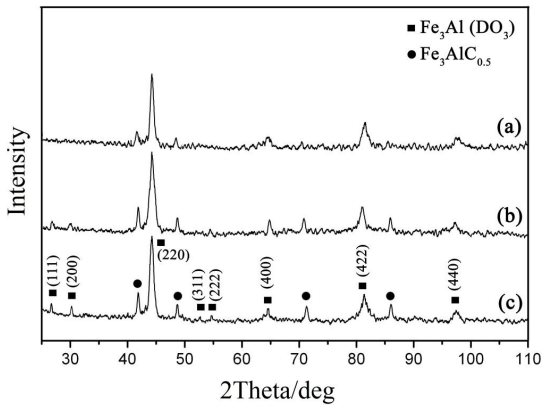


Fig. 7- XRD spectrums of Fe-28 at.% Al milled powder for different milling times of 40 (a), 70 (b) and 100 (c) hours after DSC heating.

solutions and intermetallics [24]. As illustrated in Table 1, 100 hours milling not only has induced a large amount of lattice strain in the particles but also has reduced the starting and peak temperatures of Fe<sub>3</sub>Al lattice ordering in DSC curves (Fig. 6). In other words the long time milling through increasing the lattice strain of the particles promotes the kinetics of DO<sub>3</sub>-type ordering of Fe<sub>3</sub>Al during the subsequent heating.

By calculating the area under the exothermic peaks in DSC curves of Fig. 6, the transformation enthalpies were determined as -27.17, -6.73 and -6.48 kJ/mol for the 40, 70 and 100 hours milled powders, respectively. Wang et al. [25] have theoretically calculated the formation enthalpies of disordered as well as ordered Fe<sub>3</sub>Al (Fe-28Al) as -18.04 kJ/mol and -24.88 kJ/mol, respectively. Their difference yields the ordering energy of Fe<sub>3</sub>Al as -6.84 kJ/mol which is in good agreement with the DO<sub>3</sub>-type ordering enthalpy values determined for 70 and 100 hours ball milled Fe-28Al powders in this article. These values of enthalpies appropriately support the reflections of DO<sub>3</sub>-type structure XRD peaks of the thermally analyzed samples in Fig. 7. It should be noted that the extent of the solid solution formation thus its corresponding enthalpy differs by milling time [26]. So the value of -27.17 kJ/mol calculated for the solid state transformation of 40 hours milled powder can be attributed to solid dissolution of Al in Fe and may be varied by milling time.

In Fig. 7, in addition to Fe<sub>3</sub>Al peaks, some other peaks are also observed which are corresponded to Fe<sub>3</sub>AlC<sub>0.5</sub> precipitates. The formation of these precipitates is attributed to the stearic acid which has been added as a process control agent to the powder mixture during ball milling.

Fig. 8 illustrates the DSC curves of 70 and 100 hours milled Fe-28 at.% Al powder at different heating rates. The curves in this figure exhibit an exothermic peak which as previously mentioned is associated to DO<sub>3</sub>-type ordering of Fe<sub>3</sub>Al. This ordering progresses by vacancy migration [24] which is a diffusional procedure and its accomplishment needs time. In Fig. 8 it is clearly

Table 1- Mean crystallite size and lattice strain of the synthesized Fe-28 at.% Al powder in different milling times (before DSC and after that)

Milling time (h)	Mean crystallite size (nm)		Lattice strain (%)	
	Ball milled	After DSC	Ball milled	After DSC
40	14	22	1.40	0.35
70	10	15	2.50	0.45
100	10	17	3.35	0.50

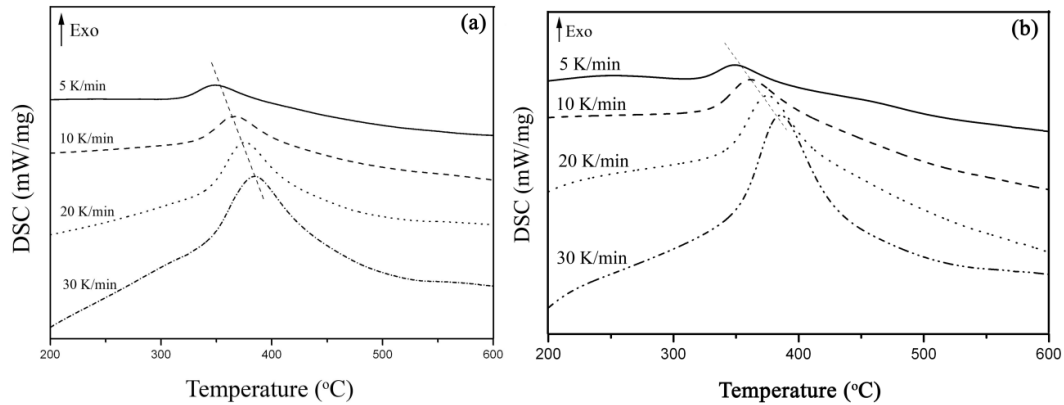


Fig. 8- DSC curves of the 70 (a) and 100 hours (b) milled Fe-28 at.% Al powder at different heating rates.

observed that through increasing the heating rate of DSC thus lack of adequate time for atomic diffusion, the exothermic peak ( $T_m$ ) has shifted to higher temperatures. The Kissinger plots for DO<sub>3</sub>-type ordering extracted from the DSC curves in Fig. 8, have been illustrated in Fig. 9. From the slope of the plotted lines in this figure, the activation energies for DO<sub>3</sub>-type ordering of Fe<sub>3</sub>Al are calculated as 156.4 and 152.1 kJ/mole for 70 and 100 hours milled powders, respectively, which are realistically higher than 31 kcal/mole (~130 kJ/mole) reported by Feder and Cahn [27]. They calculated this value based on the results of resistivity kinetics for Fe-24.8 at.% Al compound. This discrepancy is rationalized through considering the dissimilar chemical compositions and vacancy concentrations of the samples synthesized by different techniques as well as dissimilar methods used for calculation of the activation energy. Regarding the above mentioned values, the activation energy of ordering for 100

hours milled Fe<sub>3</sub>Al powder is about 4 kJ/mol lower than that for 70 hours milled powder. According to Table 1, 100 hours milling has induced about 3.35 % lattice strain in Fe<sub>3</sub>Al particles which is higher than 2.5 % for the 70 hours milled powder. It seems that the higher lattice strain due to decreasing the needed activation energy for atomic diffusion in 100 hours milled powder has decreased the activation energy for DO<sub>3</sub>-type ordering in this sample.

**4. Conclusion**

In order to synthesize the Fe<sub>3</sub>Al intermetallic compound by mechanical alloying, pure elemental powders of iron and aluminum were mixed in a planetary ball mill apparatus for up to 100 hours. Then the synthesized powders were analyzed by XRD, SEM and DSC techniques. The main extracted results are:

- 1- By increasing the milling time up to 70 hours, aluminum atoms via dissolving in bcc- iron form

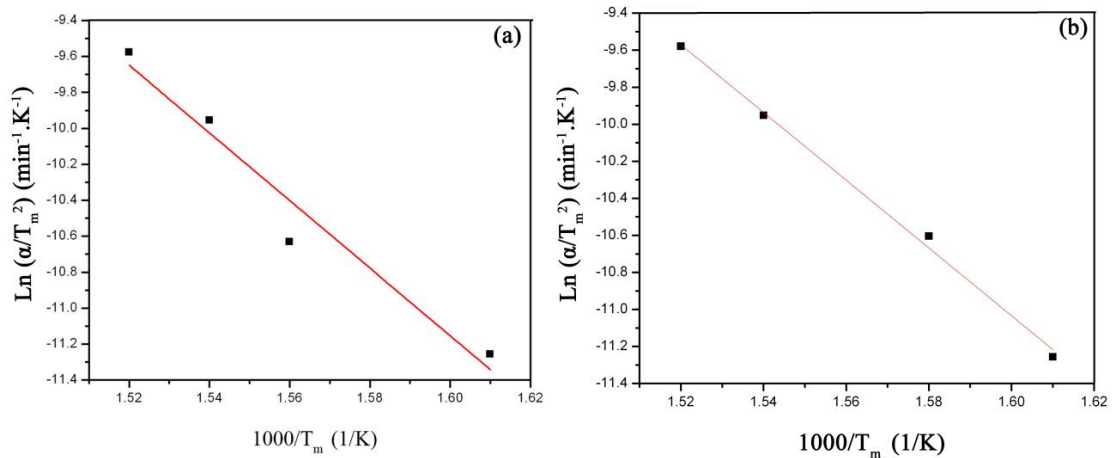


Fig. 9- Kissinger plots of DO3-type ordering in 70 (a) and 100 hours (b) milled Fe-28 at.% Al powder.

a disordered Fe(Al) solid solution. After 70 hours milling an A2-type structure of Fe<sub>3</sub>Al intermetallic compound is formed.

2- By increasing the milling time, not only the lattice strain of the particles constantly increases but also the mean crystallite and particle sizes decrease.

3- The lattice strain, mean crystallite and particle sizes of 70 hours milled powder were analytically measured as 2.5%, 10 and 500 nm, respectively.

4- Subsequent heating of 70 and 100 hours milled powders causes a DO<sub>3</sub>-type structural ordering of Fe<sub>3</sub>Al accompanied by the released heat of 6.73 and 6.48 kJ/mol, respectively. However for 40 hours milled powder, this heating only assists for the formation of disordered solid solution.

5- The activation energies of DO<sub>3</sub>-type ordering for 70 and 100 hours Fe<sub>3</sub>Al milled powder were calculated as 156.4 and 152.1 kJ/mole, respectively.

## References

- Sauthoff G. Iron Aluminides and Related Phases. Intermetallics. VCH Verlagsgesellschaft mbH. Weinheim. 1995.
- Westbrook JH, Fleischer RL. Intermetallic Compounds. Structural Applications of Intermetallic Compounds. John Wiley. 1991.
- Morris DG, Munoz-Morris MA, Baudin C. The high-temperature strength of some Fe<sub>3</sub>Al alloys. *Acta Materialia*. 2004;52(9):2827-36.
- Itoi T, Mineta S, Kimura H, Yoshimi K, Hirohashi M. Fabrication and wear properties of Fe<sub>3</sub>Al-based composites. *Intermetallics*. 2010;18(11):2169-77.
- Li YF, La PQ, Wei YP, Yang LU, Yang YA. Effect of Hot Pressing on Microstructure and Mechanical Properties of Bulk Nanocrystalline Fe<sub>3</sub>Al Materials Containing Manganese Element. *Journal of Iron and Steel Research, International*. 2011;18(3):65-71.
- McKamey CG, Liu CT. Chromium addition and environmental embrittlement in Fe<sub>3</sub>Al. *Scripta Metallurgica et Materialia*. 1990;24(11):2119-22.
- Zamanzade M, Vehoff H, Barnoush A. Cr effect on hydrogen embrittlement of Fe<sub>3</sub>Al-based iron aluminide intermetallics: Surface or bulk effect. *Acta Materialia*. 2014;69:210-23.
- Stoloff NS, Liu CT. Environmental embrittlement of iron aluminides. *Intermetallics*. 1994;2(2):75-87.
- Oleszak D, Shingu PH. Mechanical alloying in the Fe-Al system. *Materials Science and Engineering: A*. 1994;181:1217-21.
- Enayati MH, Salehi M. Formation mechanism of Fe<sub>3</sub>Al and FeAl intermetallic compounds during mechanical alloying. *Journal of Materials Science*. 2005;40(15):3933-8.
- Wang J, Xing J, Qiu Z, Zhi X, Cao L. Effect of fabrication methods on microstructure and mechanical properties of Fe<sub>3</sub>Al-based alloys. *Journal of Alloys and Compounds*. 2009;488(1):117-22.
- Peng LM, Li H, Wang JH, Gong M. High strength and high fracture toughness ceramic-iron aluminide (Fe<sub>3</sub>Al) composites. *Materials Letters*. 2006;60(7):883-7.
- Davis JR. Vol 9: Metallography and Microstructures. ASM International, Materials Park, OH. 2004.
- Bonetti E, Scipione G, Valdre G, Enzo S, Frattini R, Macri PP. A study of nanocrystalline iron and aluminium metals and Fe<sub>3</sub>Al intermetallic by mechanical alloying. *Journal of Materials Science*. 1995;30(9):2220-6.
- Farrokhi A, Samadi A, Asadi Asadabad M, Amiri Talischi L. Characterization of mechanically alloyed nano structured Fe<sub>3</sub>Al intermetallic compound by X-ray diffractometry. *Advanced Powder Technology*. 2015;26(3):797-801.
- Suryanarayana C. Mechanical alloying and milling. *Progress in Materials Science*. 2001;46(1):1-84.
- Cullity BD. Elements of X-Ray Diffraction 2nd edition. Addison-Wesley Pub. Co. Inc. 1978.
- Guinebretière R. X-ray diffraction by polycrystalline materials. John Wiley & Sons. 2013.
- Kissinger HE. Variation of peak temperature with heating rate in differential thermal analysis. *Journal of Research of the National Bureau of Standards*. 1956;57(4):217-21.
- Cahn RW. Lattice parameter changes on disordering intermetallics. *Intermetallics*. 1999;7(10):1089-94.
- Karimbeigi A, Zakeri A, Sadighzadeh A. Effect of composition and milling time on the synthesis of nanostructured Ni-Cu alloys by mechanical alloying method. *Iranian Journal of Materials Science & Engineering*. 2013;10(3):27-31.
- Rafiei M, Enayati MH, Karimzadeh F. The effect of Ti addition on alloying and formation of nanocrystalline structure in Fe-Al system. *Journal of Materials Science*. 2010;45(15):4058-62.
- Haghighi SE, Janghorban K, Izadi S. Structural evolution of Fe-50at.% Al powders during mechanical alloying and subsequent annealing processes. *Journal of Alloys and Compounds*. 2010;495(1):260-4.
- Zhu SM, Iwasaki K. Characterization of mechanically alloyed ternary Fe-Ti-Al powders. *Materials Science and Engineering: A*. 1999;270(2):170-7.
- Wang J, Xing JD, Tang HP, Yang BJ, Li YN. Microstructure and mechanical properties of Fe<sub>3</sub>Al alloys prepared by MA-PAS and MA-HP. *Transactions of Nonferrous Metals Society of China*. 2011;21(11):2408-14.
- Guilemany JM, Cinca N, Casas L, Molins E. Ordering and disordering processes in MA and MM intermetallic iron aluminide powders. *Journal of Materials Science*. 2009;44(8):2152-61.
- Feder R, Cahn RW. Kinetics of ordering in Fe<sub>3</sub>Al. *Philosophical Magazine*. 1960;5(52):343-53.